

Dynamics of 2-DOF Micro-end-Milling System Considering Grain-Size Variation

Anna Carla Araujo^{1, a}, Marcelo A. Savi^{1, b} and Pedro Manuel C. L. Pacheco^{2, c}

¹Universidade Federal do Rio de Janeiro, COPPE, Department of Mechanical Engineering, P.O. Box 68.503, 21.941.982 Rio de Janeiro, RJ, Brazil

²CEFET/RJ, Centro Federal de Educação Tecnológica Celso Suckow da Fonseca, Department of Mechanical Engineering, 20.271.110 Rio de Janeiro, RJ, Brazil

^aanna@ufrj.br, ^bsavi@ufrj.br, ^ccalas@cefet-rj.br

Keywords: End Milling, Machining Models, Modeling, Chatter.

Abstract. Non-smooth systems are employed to model different cutting processes including milling and oil drilling. This article deals with the modeling of the micro-end-milling dynamics with inhomogeneous materials. The model considers a non-smooth system composed of a primary system that represents the tool and a secondary system, representing the workpiece. This system mimics micro-end-milling dynamics considering a progressive motion of the tool holder with tool run-out. The relative position of the tool holder and the chip is evaluated avoiding huge displacements of the tool tip when the tool is not in cutting. The simplified dynamics presented in this article is used as a methodology to calculate the cutting force and tool performance from the prescribed trajectory. The inhomogeneity is related to the description of the micro-machining process where material properties cannot be considered as constant due to grain structure as the tool moves for cutting. Numerical simulations consider a situation where the workpiece is a composite with hard grains having strong differences in Young modulus comparing to matrix material. For grain distribution, microscopic analysis is employed. The main goal is to establish a qualitative comprehension of the system dynamics comparing results with homogeneous material cutting process.

Introduction

Machine tool vibrations on end-milling play an important role concerning the cutting characteristics. Dynamical behavior analysis on machining is important to improve the workpiece surface quality, avoid tool breakage and control chatter. The change of the machining parameters can control all these aspects, and the dynamics comprehension is of special interest for this aim.

In this regard, non-smooth models are employed to describe different cutting processes including machining and drilling. Non-smooth nonlinearity is usually related to discontinuous characteristics as intermittent contacts of some system components. Some related phenomena as chatter and squeal cause serious problems in many industrial applications and, in general, these forms of vibrations are undesirable because of their detrimental effects on the operation and performance of mechanical systems [1,2].

Several research efforts investigated the application of non-smooth system for different purposes. Pavlovskaja *et al.* [2] used a simplified dynamic model that is capable of qualitatively description of the behavior of an impact mechanical system with intermittent contacts and progressive drifted mass. Merritt [3] investigated the chatter on the machining process and, more recently, Gradisek *et al.* [4] and Mann *et al.* [5] treat single and two degrees of freedom systems. Reference [6] designed and modeled chatter control for turning with nonlinear single degree of freedom model using subcritical-type instability.

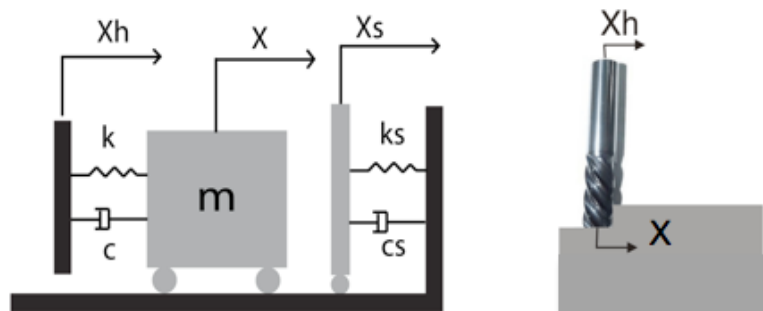
This article deals with the end-milling process modeled by a non-smooth oscillator. The idea is to describe this process by considering a one-degree of freedom oscillator operating in two different modes: contact and non-contact behaviors. Basically, the system is composed of a primary system

that represents the tool and a secondary system, representing the workpiece. Therefore, there is a discontinuity provided by a gap between the tool and the workpiece. Support properties are time dependent representing a variation of material properties. This kind of behavior is commonly found in micro-machining where the tool diameter has the same scale of the grain sizes. The cutting force is a result of a composition of contact/non-contact of the tool and the workpiece [7] and the tool holder relative displacement is predicted by the runout. The process of cutting is related to a contact behavior that defines whether the chip is being removed from the workpiece. The local force that allows the chip removal is related to the grain shear stress, which can switch from one to the other phase, being time dependent.

The grain distribution in feed direction and grain size is taken from SEM images and mechanical parameters are taken from micro-hardness tests. Under these assumptions, the equation of motion is represented by a differential equation that is solved employing the Runge-Kutta method. Numerical simulations are carried out for two-grain distributions, establishing a qualitative comparison with homogeneous material.

Dynamic Model

The milling process is of concern by considering a full immersed milling in the feed direction [8]. This process is modeled by assuming a non-smooth system composed of a primary system that represents the tool and a secondary system, representing the workpiece. Fig. 1a shows the general view of the tool and the workpiece where it is identified the prescribed displacement, X_h and the tool tip displacement, X .



(a) Systems Model (b) Tool Displacements

Figure 1. Tool and System Modeling

The primary system consists of a linear mass-spring-dashpot oscillator with parameters m , k , c and displacement X . There is a gap that separates itself from the secondary system that represents the workpiece. The workpiece system is represented by a spring-dashpot system with parameters k_s , c_s , without mass, and the displacement is denoted by X_s .

The system may operate in contact/non-contact situations, and therefore, its nonlinear dynamics is associated with non-smooth equations [7]. Note that the system is in a non-contact mode when the displacement is less than the gap. Otherwise, the system is in contact mode that represents the cutting stage.

The difference between X_s and X represents the chip removal. Similarly as in [1], the contact conditions can be defined as follows:

$$h_\alpha(X) = X - g > 0 \quad (1)$$

$$h_\beta(X, \dot{X}) = -(X - g) - \frac{c_s}{k_s} \dot{X} < 0 \quad (2)$$

When X is less than the gap and h_α is less than zero (Eq.1) or the force retracts the tool and h_β is greater than zero (Eq.2), the system remains in the non-contact mode. In the phase space shown in Fig. 2 these transitions are related to a hyper-surface that consists of the conjunction of two surfaces Σ_α and Σ_β . The hyper-surface Σ_α defines the transition from Γ_- to Γ_+ , representing situations where the contact is caused when X becomes greater than g . On the other hand, the hyper-surface Σ_β defines the transition from Γ_- to Γ_+ as the contact is lost when the force of the support vanishes. The support relaxes to the equilibrium state when there is no contact between the mass and the support.

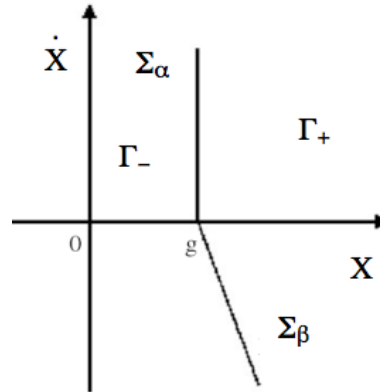


Figure 2. Subspaces related to the system dynamics of a non-smooth system [1].

Model Equations. The equations of motion are represented by a non-smooth system that has two operation modes: contact and non-contact. In non-contact mode, the secondary system does not present any movement and its displacement does not change. The primary system is described by the dynamic equation of a single-degree of freedom system:

$$m\ddot{X} + c\dot{X} + kX = c\dot{X}_h + kX_h \quad (3)$$

In contact mode, the chip is removed reacting to the tool and the system is described by:

$$m\ddot{X} + (c + c_s)\dot{X} + (k + k_s)X = c\dot{X}_h + kX_h + k_s g \quad (4)$$

Therefore, the system dynamics is governed by two different equations and the state space is split into two parts associated with contact and non-contact behaviors, as shown in Fig. 2.

System Parameters. The machine tool and the tool holder have a prescribed displacement X_h around the feed velocity trajectory. This variation is a function of the spindle speed ω and the amplitude ρ , representing the run-out around the spindle axis. All these aspects are considered by assuming a harmonic function as follows:

$$X_h(t) = \rho \sin(\omega t) \quad (5)$$

Non-dimensional parameters can be used in order to define dynamic characteristics. Eq. 6 introduces the relations for ω_o , r_Ω , ξ and r_c .

$$r_\Omega = \frac{\omega}{\omega_o} ; \quad \xi = \frac{c}{2m\omega_o} ; \quad r_c = \frac{c_s}{c} ; \quad \omega_o = \sqrt{\frac{k}{m}} \quad (6)$$

In order to represent micro-milling processes, the workpiece properties depend on the grain material. A possible way to model this dependence is to treat the support properties, k_s and c_s , as a time dependent or displacement dependent function. Microscopic analysis can be employed to define this function.

Numerical Simulations

Numerical simulations are carried out in order to establish a qualitative comparison between homogenous and non-homogeneous material dynamic behavior. The governing equations are solved using a fourth order Runge-Kutta method with a time step less than 1/100 of the spindle cycle.

It is assumed that the gap vanishes and the tool damping is 0.002 N s/m for both materials. End-milling parameters presented in [9] are employed with 508 μm diameter tool with 2 flutes, 10 mm long, and the conditions listed in Table 1. Non-dimension parameters are: $\zeta=0.01$, $r_Q=0.8$ and $r_c=1000$. Feed rate (ft) is 10 $\mu\text{m}/\text{flute}$.

Table 1. Machining Parameters

Spindle Speed (n)	84.000 rpm
Tool runout (ρ)	1 μm
Axial Depth of Cut (b)	100 μm

Simulation with homogeneous workpiece

First, simulation considers a homogeneous workpiece. The workpiece material is simulated based on microscopy and micro-hardness tests taken from literature. A duplex stainless steel 60-40 [10] is taken as a reference material. For this material austenite and ferrite present Young modulus values of 182 ± 14 GPa and 204 ± 7 GPa, respectively, whereas the intermediate phase presents a value of 187 ± 13 GPa. In this article a value of 180 GPa is considered.

Fig. 3 presents the phase space diagram for two different feed velocities. It can be seen that a similar dynamic behavior for the two feed velocities.

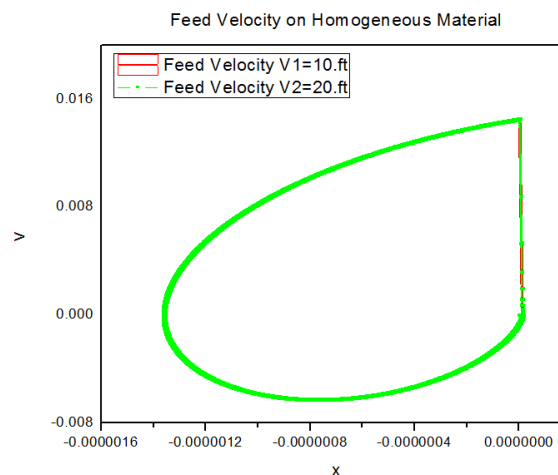


Figure 3. Phase Space for Homogenous Material using two different feed velocities.

Fig. 4 shows a representation of the contact and non-contact behavior of the tool engaged on the workpiece, respectively represented by 1 or 0. A value of 1 represents a situation where the grain is in contact with the tool. It can be seen that the contact stage is equally distributed on time.

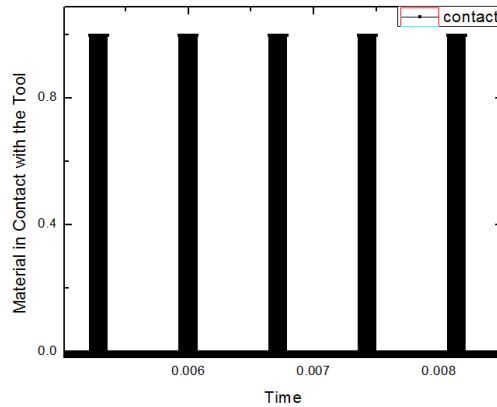


Figure 4. Contact and Non-contact Analysis.

Material Distribution Patterns with Different Hard Grain Sizes

The grain structure is organized intercalated by two different materials, with stiffness values of k_{s1} and k_{s2} , in feed direction, beginning at the first contact point, as shown in the Fig. 2. The damping coefficients are assumed to be the same for both materials. The work-piece length in feed direction is divided in subsets containing a pattern with different grains. Fig. 5 presents one pattern with repeated grain sizes $L1$ and $L2$ composing the cell size Lc .

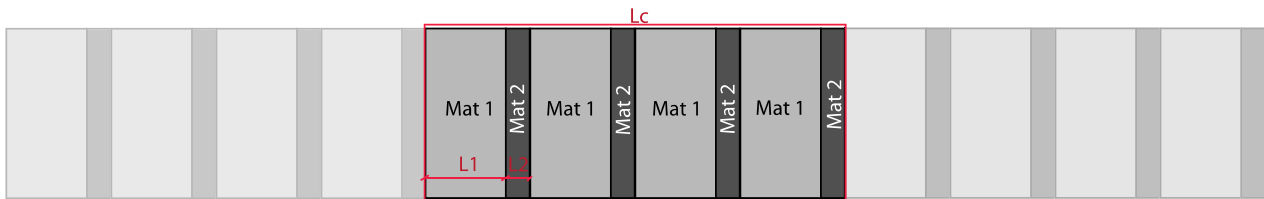
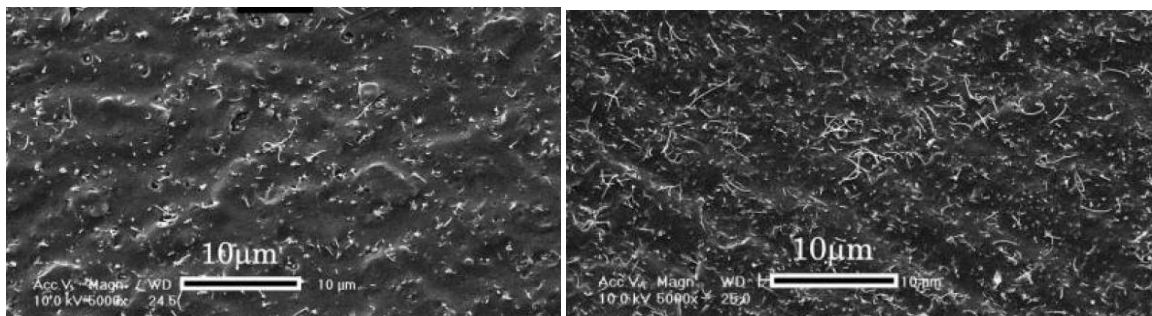


Figure 5. Cell Pattern in Feed Direction

As it was claimed, Young modulus for Material 1 is considered as 180 GPa. The second material, Material 2, can be either the second phase of the super-duplex stainless steel or a hard grain added to this structure. For example, a material as a Poly[styrene-*b*-(ethylene-cobutylene)-*b*-styrene] as matrix material can receive Pristine MWCNTs as a hard material in the composite as shown in Fig. 6 [11]. To study the effect of the presence of dissimilar materials in the workpiece on the dynamic behavior the following simulations considers that Material 2 has a Young modulus three orders of magnitude larger than the one for Material 1.



(a) 1.25 wt% CNT Loading

(b) 2.5 wt% CNT Loading

Figure 6. SEM images of SEBS/MWCNT nanocomposites [11].

Two regular patterns and one irregular pattern were created to analyze the influence of the hard grain size. Pattern A has the cell size L_c equals to $30\ \mu\text{m}$. Inside this pattern repetition, material A has $6.5\ \mu\text{m}$ grain (L1) and the hard material has $1\ \mu\text{m}$ grain size (L2). Pattern B has $4.5\ \mu\text{m}$ grain size (L1) with $3\ \mu\text{m}$ hard grains (L2), regularly distributed. Pattern C is a irregular distribution with repetition of the following composition: $4.5\ \mu\text{m}$, $3\ \mu\text{m}$, $2\ \mu\text{m}$, $6\ \mu\text{m}$, $3\ \mu\text{m}$ and $4\ \mu\text{m}$ grains of matrix material (L1) with $1\ \mu\text{m}$ hard grain size (L2) between them.

Figs. 7 and 8 present phase space diagrams for homogeneous workpiece and patterns A, B and C considering two feed velocities. Results show that the three hard grain materials present a dynamic behavior with thicker band orbits in comparison with the homogeneous material. This behavior is associated to larger oscillations within the orbits and can affect the workpiece surface finish. Fig. 8 shows that for larger velocities, the dynamic of the workpiece machining is more similar to the homogeneous as less thick band orbits are observed.

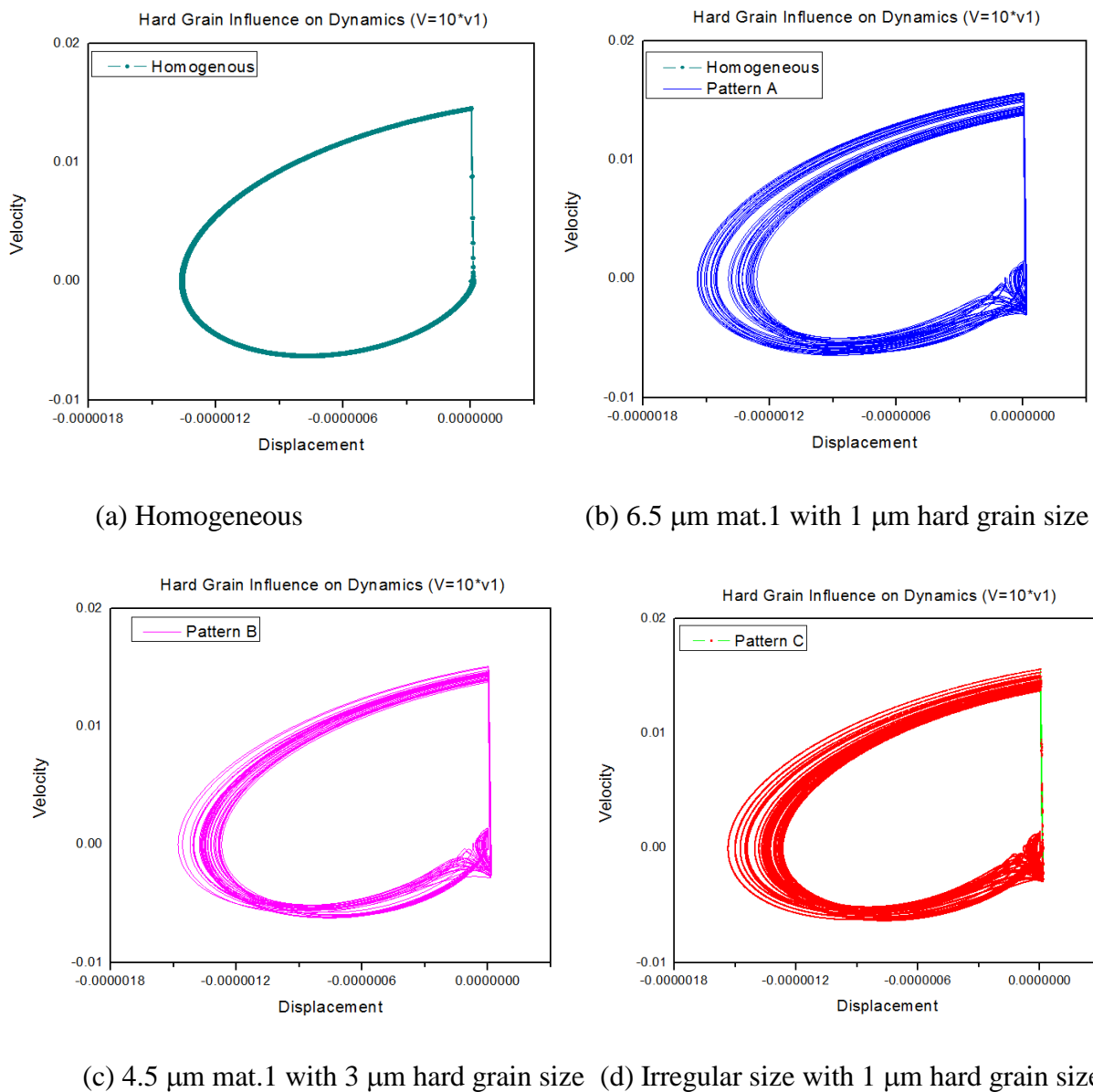
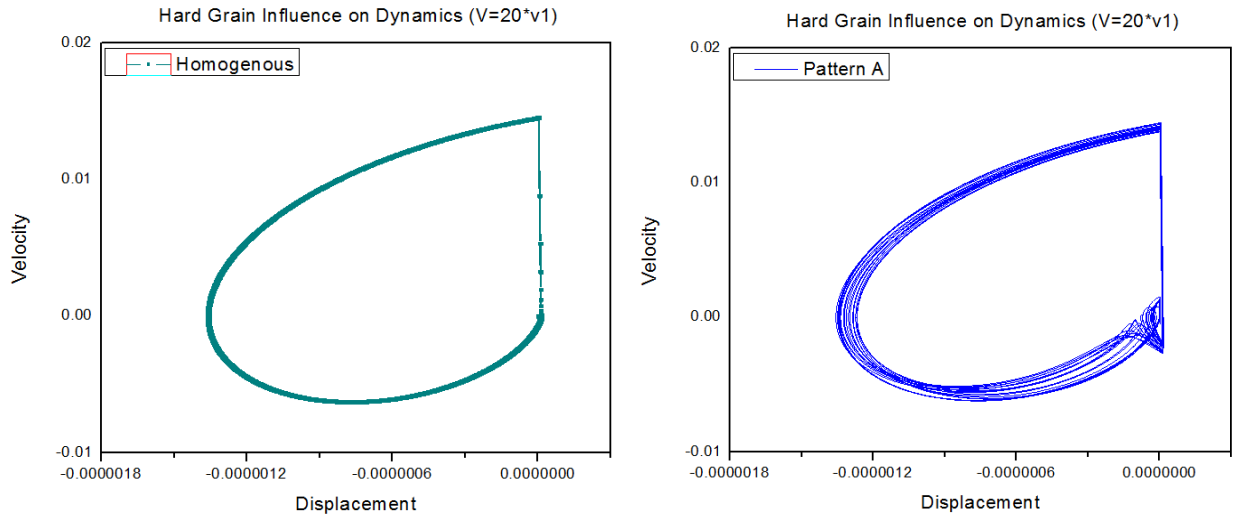
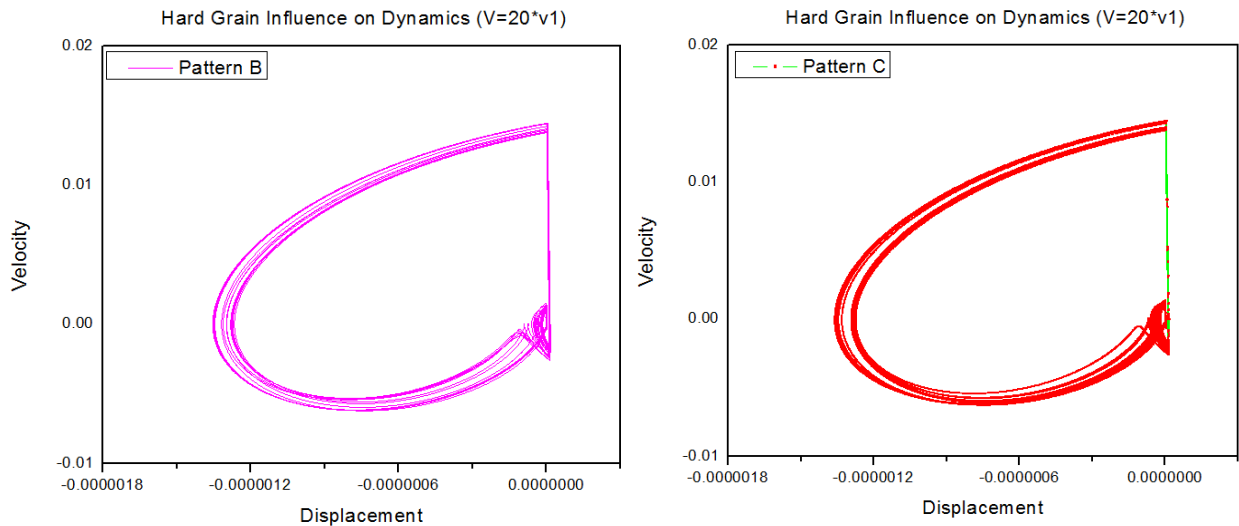


Figure 7. Phase Space machining materials with $V=10 \cdot v_1$.



(a) Homogeneous

(b) 6.5 μm mat.1 with 1 μm hard grain size



(c) 4.5 μm mat.1 with 3 μm hard grain size (d) Irregular size with 1 μm hard grain size

Figure 8. Phase Space machining materials with $V=20$ ft.

Fig. 9 presents the contact and non-contact behavior for the three different patterns considering $V=10$ ft. Different behaviors are observed for the three patterns. Pattern B has similar grain sizes and the tool maintains contact with the material whereas the other two patterns present larger periods of non-contact.

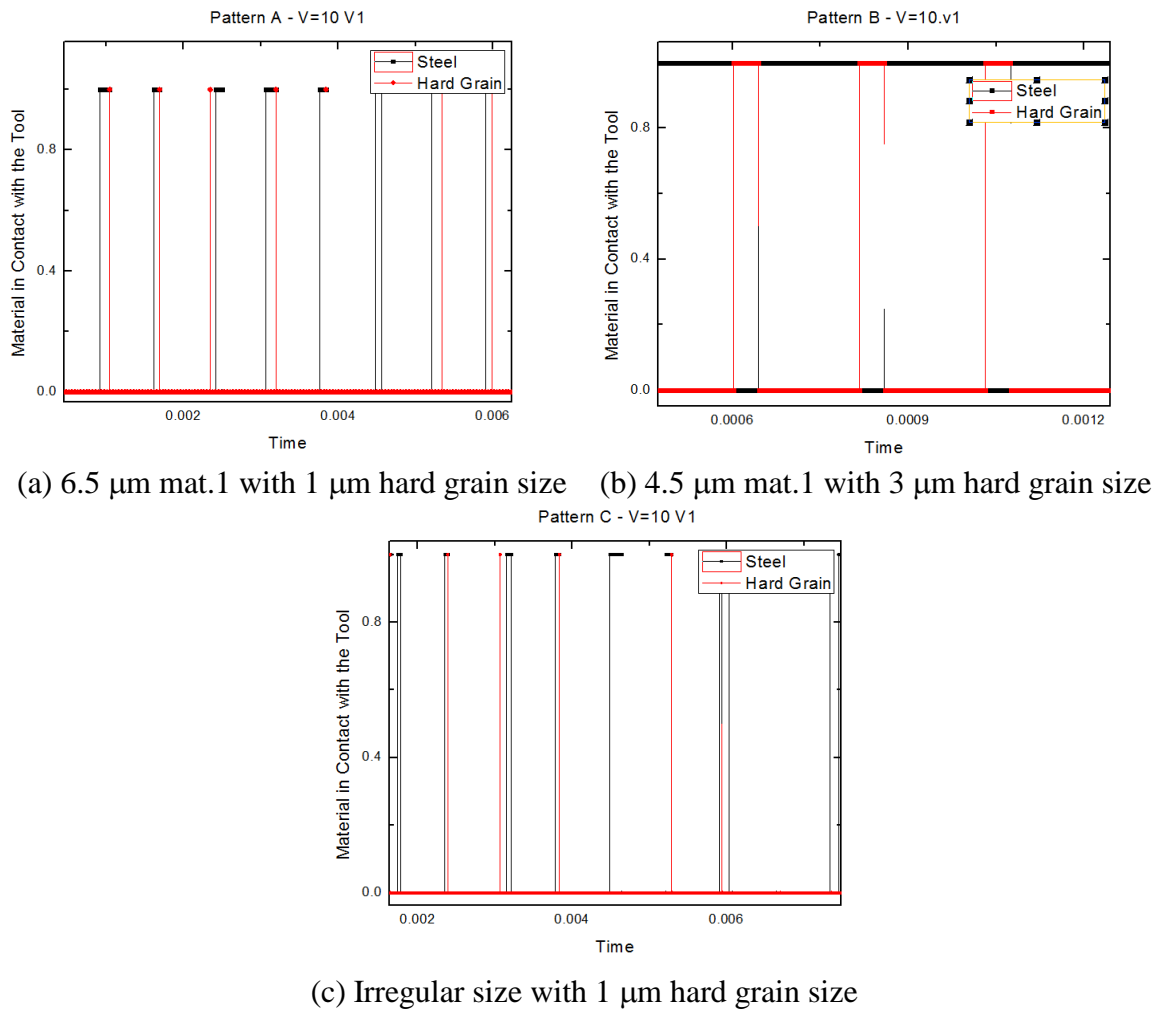


Figure 9. Contact and Non-contact Tool and Material Analysis.

Conclusions

This paper discusses the modeling and simulation of the micro-end-milling dynamics. A one-degree of freedom non-smooth oscillator is employed to describe the system dynamics. Basically, it is established a qualitative comparison between homogeneous and non-homogeneous material showing the main differences in dynamical response. The proposed model can be useful to choose important parameters to improve tool behavior.

References

- [1] M.A. Savi, S. Divenyi, L.F.P. Franca and H.I. Weber: J. of Sound & Vib. Vol. 301 (2007), pp. 59-73.
- [2] E.E.,Pavlovskaja, M. Wiercigroch and C. Grebogi: Phys. Rev. E Vol. 64 (2000), pp. 1-9.
- [3] H. Merritt: J. Eng. for Ind. Vol. 87 (1965), pp. 447-454.
- [4] J. Gradisek, M. Kalveram, T. Insperger, K. Weinert, G. Stépán, E. Govekar and I. Grabec: Int. J. Mac. Tools & Man. Vol. 45 (2005), pp. 769-781.
- [5] B.P. Mann, N.K. Garg, K.A. Young and M. Helvey: Nonlinear Dyn. Vol. 42 (2005), pp. 319-337.
- [6] J.R. Pratt and A.H. Nayfeh: Nonlinear Dyn. Vol. 19 (1999), pp. 49-69.

-
- [7] A.C. Araujo, P.M.C.L. Pacheco and M.A. Savi: Dynamical Analysis of an End Milling Process, COBEM 2009 (2009).
- [8] A.C. Araujo, M.A. Savi and P.M.L.C. Pacheco: Experimental and Numerical Dynamical Analysis of an End Milling Process, CONEM 2010 (2010).
- [9] M. Jun: Modeling And Analysis Of Micro-End Milling Dynamics, Ph.D. Thesis in University of Illinois at Urbana-Champaign (2005).
- [10] M. Campos, A. Bautista, D. Cáceres, J. Abenojar and J.M. Torralba: J. of Eur. Cer. Soc. Vol. 23 (2003), pp. 2813-2819.
- [11] Z. Spitalskya, D. Tasisb, K. Papagelisb, and C. Galiotis: Progress in Polymer Science Vol. 35 (2010), pp. 357-401.